Available online at www.sciencedirect.com
ScienceDirect
Biosensors and Bioelectronics 22 (2007) 3028–3035
BIOSENSORS & BIOELECTRONICS
www.elsevier.com/locate/bios

Microresonator mass sensors for detection of *Bacillus anthracis* Sterne spores in air and water

Angelica P. Davila [a], Jaesung Jang [a], Amit K. Gupta [a,1], Tom Walter [b], Arthur Aronson [b], Rashid Bashir [a,c,*]

[a] *Laboratory of Integrated Biomedical Micro/Nanotechnology and Applications, Birck Nanotechnology Center, Bindley Biosciences Center, School of Electrical and Computer Engineering, Purdue University, West Lafayette, IN 47907, United States*
[b] *Department of Biological Sciences, Purdue University, West Lafayette, IN 47907, United States*
[c] *Weldon School of Biomedical Engineering, Purdue University, West Lafayette, IN 47907, United States*

Received 12 September 2006; received in revised form 21 December 2006; accepted 5 January 2007
Available online 25 January 2007

Abstract

Towards the goal of developing a real-time monitoring device for microorganisms, we demonstrate the use of microcantilevers as resonant mass sensors for detection of *Bacillus anthracis* Sterne spores in air and liquid. The detection scheme was based on measuring resonant frequency decrease driven by thermally induced oscillations, as a result of the added mass of the spores with the use of a laser Doppler vibrometer (LDV). Viscous effects were investigated by comparing measurements in air and deionized (DI) water along with theoretical values. Moreover, biological experiments were performed which involved suspending spores onto the cantilevers and performing mass detection in air and water. For detection of spores in water, the cantilevers were functionalized with antibodies in order to fix the spores onto the surface. We demonstrate that as few as 50 spores on the cantilever can be detected in water using the thermal noise as excitation source. Measurement sensitivity of 9.23 Hz/fg for air and 0.1 Hz/fg for water were obtained. These measurements were compared with theoretical values and sources of improvement in cantilever sensitivity in a viscous medium were also discussed. It is expected that by driving the cantilevers and using higher order modes, detection of a single spore in liquids should be achievable.

Keywords: Microcantilever; Resonant mass sensor; Spore detection; Viscous medium

1. Introduction

During the last decade, a number of biosensors have been developed to perform measurements and detection of microorganisms for a variety of applications such as food analysis, clinical diagnostics, and environmental monitoring (Ivnitski et al., 1999). Current methods of detection and identification of pathogens include plate culture, polymerase chain reaction (PCR), and enzyme-linked immunosorbent assay (ELISA). While these types of tests are well established and can accurately identify pathogens, they tend to be laborious and time-consuming requiring days for accurate identification (Ivnitski et al., 1999; Burtscher and Wuertz, 2003; Prescott et al., 2005). The need for a sensor that accurately detects a few cells in a label free manner and in real time has prompted researchers to use cantilevers as mass sensors. Cantilever sensors (Lavrik et al., 2004) generally measure the change of deflection or resonant frequency shifts to detect the target analyte. The latter type of cantilever sensor will be discussed in the current study. The general principle of these cantilever mass sensors can be expressed by the following equation for added mass as:

$$\Delta m = \frac{k}{4n\pi^2}\left(\frac{1}{f_1^2} - \frac{1}{f_0^2}\right), \quad (1)$$

where k is the spring constant, $n = 1$ if the mass is placed at the free end, f_1 is the resonant frequency due to the added mass and f_0 is the resonant frequency without the mass (Gupta et al., 2004a).

* Corresponding author. Tel.: +1 7654966229.
E-mail address: bashir@purdue.edu (R. Bashir).
[1] Present address: BioMEMS Resource Center, Center for Engineering in Medicine, Massachusetts General Hospital, Shriners Hospital for Children and Harvard Medical School, Boston, MA 02114, United States.

0956-5663/$ – see front matter © 2007 Elsevier B.V. All rights reserved.
doi:10.1016/j.bios.2007.01.012

One of the earliest uses of cantilevers as mass sensors of micro-sized particles was detection of the mass of 10 μm diameter latex beads using silicon dioxide cantilevers. In this study, the sensors exhibited a minimum detectable mass of approximately 0.2 ng (Prescesky et al., 1992). It was also one of the first demonstrations of the cantilever as a biosensor. Detection of bacteria and viruses in air has also been reported, with the mass of a single cell of the bacterium *Escherichia coli* (*E. coli*) reported as 665 fg (Ilic et al., 2001) and a single vaccinia virus as 9.5 fg (Gupta et al., 2004b). Single particle detection was a milestone for cantilever mass sensors, but these measurements were performed in air. On the other hand, detection of few cells on the cantilevers in liquid has been difficult to realize because of large damping in liquid and the resulting decrease in the quality factor.

Recently, mass detection of latex beads using biotin–streptavidin interactions was performed by quantifying the resonant frequency shifts at higher order harmonic frequencies (Braun et al., 2005). Promising features of this work included the real-time monitoring of mass detection in liquid of an adsorbed mass of 7 ng with sensitivity of 2.5 pg/Hz. Additional studies have demonstrated the use of cantilevers to detect and monitor the growth of *E. coli* cells and fungal spores (*Aspergillus niger*) (Gfeller et al., 2005; Nugaeva et al., 2005). In these studies, the cantilevers were functionalized with nutrient media that induced the growth of bacteria and spores captured onto the surface of the cantilever. For *E. coli* detection, the sensitivity of these cantilevers was approximately 140 pg/Hz, corresponding to about 200 bacterial cells (Gfeller et al., 2005) and for detection of the fungal spores, the sensitivity was 1.9 pg/Hz, resulting in the ability to detect a minimum of about 60 fungal spores in a humid air environment (Nugaeva et al., 2005). Millimeter-sized piezoelectric-excited cantilevers were also used to specifically detect *Bacillus anthracis* spores at a concentration of about 300 spores/mL in liquid medium (Campbell and Mutharasan, 2006).

For real-time biological detection in liquid, a novel hollow microcantilever has been reported in which the liquid flows inside the cantilever, allowing measurement of the changes in resonant frequency to be done in air (Burg and Manalis, 2003). Mass sensitivity of 0.1 Hz/pg was reported and since this architecture does not compromise the quality factor (Q) of the cantilever, much higher sensitivities should be possible. The quality factor is a measure of energy dissipation of the cantilever and is directly related to the sensitivity since the higher the Q, the smaller the minimum detectable frequency and the smaller the minimum detectable mass. The hollow cantilever maintains the high Q obtained by operating in air but can still perform real-time measurements in liquid by introducing the liquid inside the cantilever. However, because of the architecture of the cantilever, viewing and imaging the adsorbates on the channel surface is not possible.

In general, cantilever sensors are promising due to their small size, high sensitivity, and ability for real-time measurements and mass production. For biological detection, it is often necessary to be able to perform quantitative measurements in an aqueous environment, where the sensitivity of the resonant cantilevers greatly decreases due to large damping. Therefore, the ability to detect a small number of microorganisms is hampered. In this paper, we explore the feasibility of using cantilevers as mass sensors to detect microorganisms in air and liquid using thermal noise driven oscillations. This results in quality factors of less than 5 in water. We use DI water as a viscous liquid. By measuring the resonant frequency of the cantilevers before and after the binding of the spore particles, their mass can be determined. First, known masses are attached to the tip of the cantilever in order to investigate and observe viscous effects in liquid. Next, *B. anthracis* Sterne spores are used to perform the biological detection studies. We also compare these measurements with theoretical estimates and discuss several ways to improve the mass sensitivity and minimum detectable mass of the cantilevers.

2. Materials and methods

2.1. Cantilevers and instrumentation

The cantilevers used for this study were fabricated using silicon-on-insulator (SOI) wafers and standard surface micromachining techniques as described earlier (Gupta et al., 2004b). The chip consists of two channels with nominal cantilever lengths of 100, 75, 50, 40 and 20 μm and uniform width and thickness of 9 μm and 200 nm, respectively (see Fig. S1). Detailed information on preparation steps and instruments are in the supplementary text.

2.2. Characterization of the cantilevers with silica beads

To perform detection of a known mass in liquid, silicon dioxide beads with diameters of 5.06 and 3.5 μm were used (Bangs Laboratories Inc., Fishers, IN USA). The beads were non-porous so that they would not absorb any fluids to alter their real mass, which was important since the measurements were to be performed in liquid. Detailed measurement procedure is in the supplementary text.

2.3. Measurements of the spores in air

For the spore measurements in air, a glass cover was placed over the stage where the chip was located with a nitrogen gas flow through the glass. The purpose of this was to try to minimize the effect of the humidity in the ambient room air. Next, 20 μL of *B. anthracis* Sterne spores [conc. 10^9 spores/mL] was introduced onto the chip and the spores were allowed to settle on the surface of the cantilevers for 4 h. The chip was then dried with the CPD and the resonant frequency measurements were performed in air with the spores on the cantilevers.

2.4. Spore immobilization and measurements in water

First the cantilever chip was piranha-cleaned, dried with CPD, and oxygen plasma etched to remove any residual organic contaminants. In order to perform the unloaded resonant frequency measurements, a ring of silicone rubber was placed onto the chip and 50 μL of DI water was added onto the chip. A glass

cover slip was placed over the chip and the unloaded resonant frequency in water was measured with the LDV.

After the measurements, the chip was dried with the CPD and the cantilevers were functionalized with antibodies. First, the chips were incubated for one hour in 20 μL of *B. anthracis* spore antibody [conc. 1.15 mg/mL] obtained from USBiological (Swampscott, MA). The chip was then rinsed in phosphate buffered saline (PBS) for 30 s. After rinsing in PBS, 20 μL of bovine serum albumin (BSA) [conc. 5 mg/mL] was added onto the chip for 15 min. BSA was used to prevent non-specific binding of other contaminants onto the cantilever. Next, the chip was rinsed in PBS with 0.05% Tween for 30 s in order to remove any excess antibodies that were not attached. The chip was prepared for the CPD by immersing it in different concentrations of methanol and PBS starting from 20% methanol in PBS increasing to 100% methanol. The chip was dried with the CPD, and the resonant frequency measurements due to the antibody and BSA were performed in air. Following the measurements in air, measurements in water were performed. First, a new silicone rubber was placed on the chip and the antibodies were rehydrated by adding 10 μL of PBS to the experimental channel for approximately one minute. Then, 55 μL of sterile DI water was placed on the chip along with a glass cover slide, and frequency measurements in water were performed.

After the antibody/BSA measurements, the spores were added to the chip. The PBS was rinsed off with DI water. Then, 20 μL of *B. anthracis* Sterne spore solution [conc. 10^9 spores/mL] was introduced over the channel and allowed to settle for 16 h. The chip was then dried with the CPD along with the same increasing concentration of methanol in PBS as previously mentioned. After the CPD, the frequency measurements were performed in air with the spores attached to the cantilevers. Lastly, the loaded frequency measurements were performed in water. These frequency measurements in water and air will be used to compare with the frequency measurements due to the antibody/BSA and compute the mass of the spores.

3. Results and discussion

3.1. Viscous effects on the dynamic response

Characterization of the dynamic behavior of cantilevers in fluids has been explained with several models. One of these models is the inviscid model, which can be described by

$$\frac{\omega_{\text{fluid}}}{\omega_{\text{vac}}} = \left(1 + \frac{\pi\rho_{\text{f}} b}{4\rho_{\text{c}} t}\right)^{-0.5}, \tag{2}$$

where ω_{fluid} is the radial resonant frequency in fluids, ω_{vac} is the radial resonant frequency in vacuum, ρ_{f} is the density of the fluid, b and t are the width and thickness of the cantilever, respectively, and ρ_{c} is the density of the cantilever (Chu, 1963). Because this model does not take account of viscous effects, significant errors may arise in the prediction of the resonant frequency in micro/nano cantilevers, although it has been shown to work well for macroscopic cantilevers or large Reynolds number cases (Chon et al., 2000). Sader (1998) presented a theoretical analysis of the frequency responses of a uniform cantilever beam immersed in a viscous fluid and excited by thermal noises. This viscous model approximates to a simpler form, a simple harmonic oscillator (SHO) model, in the limit of large quality factors, where the resonant frequency is given by

$$\omega_{\text{vac},n} = \omega_{R,n}\left(1 + \frac{\pi\rho_{\text{f}} b}{4\rho_{\text{c}} t}\Gamma_{\text{r}}\left(\omega_{R,n}\right)\right)^{0.5}, \tag{3}$$

where $\omega_{R,n}$ is the radial resonant frequency of mode n in the absence of dissipative effects, and Γ_{r} is the real part of the hydrodynamic function that depends on fluid viscosity (Sader, 1998). The inviscid model leads to large discrepancies due to the fact that viscous effects are not taken into account while the SHO model is in close agreement with the measured resonant frequencies (see Fig. S2).

The frequency responses of cantilevers immersed in a viscous fluid can also be estimated by the quality factor, which is given in the SHO model by

$$Q_n = \left[\frac{(4\rho_{\text{c}} t/\pi\rho_{\text{f}} b) + \Gamma_{\text{r}}(\omega_{R,n})}{\Gamma_{\text{i}}(\omega_{R,n})}\right], \tag{4}$$

where Q_n is the quality factor of mode n and Γ_{i} the imaginary part of the hydrodynamic function (Sader, 1998). This model was reported to be valid at $Q_n \geq 1$ and the length to width ratio larger than 4 (Chon et al., 2000). As the viscous damping of the surrounding fluids increases, the frequency spectrum broadens indicating that the quality factor decreases. Therefore, a large frequency shift is required in order to resolve between two signals, and hence the minimum added mass that can be detected increases. That is, the minimum detectable frequency shift and minimum detectable mass increase. The minimum detectable frequency shift is expressed by

$$\Delta f_{\text{min}} = \frac{1}{\langle z^2\rangle^{1/2}}\sqrt{\frac{f_0 k_B T B}{2\pi k Q}} \tag{5}$$

where $\langle z^2\rangle^{1/2}$ is the square root of the mean square amplitude of the cantilever, k_{B} is Boltzmann's constant, T is temperature, B is the measurement bandwidth, and k is the spring constant of the cantilever (Ekinci et al., 2004).

Fig. 1 shows the quality factors obtained from the unloaded frequency measurements and the theoretical values predicted by the SHO model in air and DI water. It was observed that deviations of the theoretical predictions from the measurements decrease with the increasing length in both air and water. These deviations are mainly because the theoretical model was developed based on the large length to width ratios. According to this graph, this SHO model overestimates the quality factor in shorter cantilevers.

3.2. Measured mass of the beads in air and water

The 3.5 μm beads had a standard deviation of 0.35 μm in diameter resulting in an expected mass of 32.1 to 58.6 pg (using a density of 1.96 g/mL). The beads were attached using the procedure described in Section 2. The cantilevers were imaged by

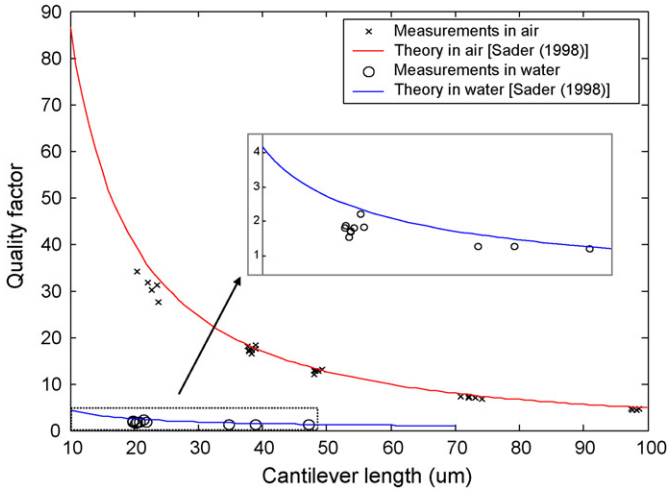

Fig. 1. Measured quality factors in air and DI water with theoretical calculations based on the SHO model (Sader, 1998). Cantilever width = 9 μm and cantilever thickness = 200 nm.

SEM in order to count the beads on the surface. On some occasions, more than one bead was picked up by the probe and added to the cantilever tip. The average measured mass of the 3.5 μm bead in air was 31.2 pg, which was very close to the expected value, as shown in Table 1(a). The mass of the epoxy was also measured and resulted in an average measured mass of 4.3 pg.

Measurements in water were then performed using the two cantilever lengths, as shown in Table 1(a). The average mass of the beads was found to be 116.3 pg. Although the mass of the dry beads was about 35 pg per bead, the extracted mass in water using Eq. (1) was about 85 pg greater. This difference can be attributed to the induced mass effect where the mass of the fluid around the cantilever and the bead are contributing to the total mass measured in water. This phenomenon is explained below.

3.3. Induced mass effects in fluids

It is well known that when a structure is vibrating in a viscous fluid, it experiences damping as well as an additional force by the surrounding fluid as if an additional mass were attached to the structure (Chen, 1987), resulting in a loss of the mass sensitivity of the cantilevers (Braun et al., 2005). This induced mass, m_L, is expressed as

$$m_L = pm_d = p\rho_f V_c, \tag{6}$$

where p is the added mass coefficient, m_d is the displaced mass, and V_c is the volume of the structure (Chen, 1987; Kirstein et al., 1998; Braun et al., 2005). For a perfect fluid whose damping is zero, the only resistance encountered by the structure is the fluid inertia, or the induced mass.

The induced mass for an oscillating sphere of an effective radius R is given by

$$m_L = \frac{4}{3}\pi R^3 \rho_f \left(\frac{1}{2} + \frac{9}{4}\sqrt{2\left(\frac{\omega R^2}{\nu}\right)^{-1}}\right), \tag{7}$$

where ν is the kinematic viscosity of fluid, and ω is the radial frequency of a sphere (Landau and Lifshitz, 1959). For a rectangular cantilever, the added mass coefficient is given by

$$p = 1 + \frac{4}{\sqrt{2Re}}, \tag{8}$$

where $Re = \omega b^2/\nu$ is the Reynolds number (Kirstein et al., 1998). As shown in these two expressions above, the added mass coefficient is a function of the Reynolds number for a given vibrating geometry. The Reynolds number is the ratio of the inertia force to the viscous damping force. Therefore, the induced mass increases with the viscosity of fluid as well as the displaced mass. This is also observed in Fig. 2, which shows the measured added mass coefficient of the cantilevers in water as a function of the Reynolds number together with the theoretical predictions (Kirstein et al., 1998). The measurements are shown to be in good agreement with the theoretical prediction.

3.4. Spore detection in air

All five cantilever lengths were used in this experiment, but the number of spores captured on the cantilever surface was small and the longer cantilevers were not sensitive enough to exhibit a significant shift in frequency for given added masses. We observed a frequency shift in the three cantilevers with lengths of 50, 40 and 20 μm. The data were analyzed using Matlab software to extract the resonant frequencies and quality factors by fitting the measured thermal spectra to the amplitude response of a simple harmonic oscillator (Walters et al., 1996). The spring constant was also extracted using the Sader method (Sader et al., 1999).

The spores were imaged by SEM and the effective number of spores was counted for each of the cantilevers (see Fig. S3). The effective number of spores was obtained by multiplying each spore by a factor of x/l, where x was the distance from the fixed end to each spore and l was the length of the cantilever beam (Ilic et al., 2001; Gupta et al., 2004a). In order to account for the spores found on the bottom of the cantilevers, it was assumed

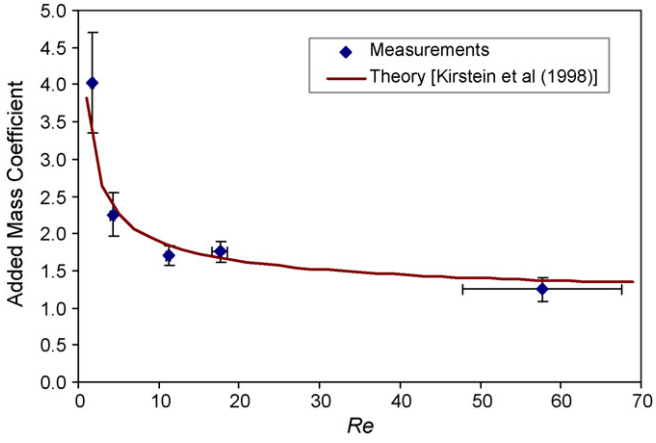

Fig. 2. Measured added mass coefficients in DI water with theoretical values as a function of the Reynolds number. The error bars indicate 95% confidence intervals. Cantilever width = 9 μm and cantilever thickness = 200 nm.

Table 1
Measured mass of 3.5 μm silica beads in air and DI water (a) and measured mass of spores in air (b) and DI water (c)

(a)

Cantilever	Length (μm)	Total measured mass change		Effective no. beads	Mass of a bead in air (pg)	Mass of a bead in water (pg)
		In air (pg)	In water (pg)			
L31	37.80	29.01	114.07	1	29.01	114.07
L32	38.40	61.21	326.04	1	NA	NA
L33	37.95	31.13	162.15	1	31.13	162.15
L34	38.25	29.45	43.08	0.946	31.13	45.53
L35	38.85	79.58	113.03	2.69	29.58	42.02
L36	38.85	39.39	72.88	1	39.39	72.88
L37	37.65	13.14	89.95	Glue		Glue
L39	37.95	29.60	193.87	1	29.60	193.87
L41	23.57	67.45	186.81	2	33.12	93.41
L43	20.40	30.10	124.44	1	30.10	124.44
L45	22.80	28.84	186.94	1	28.84	186.94
L47	22.20	29.79	110.00	1	29.79	110.00
L49	23.71	62.40	267.80	2	31.20	133.90
Average mass (pg)					31.17	116.29
Standard deviation (pg)					2.99	49.05

(b)

Cantilever	Length (μm)	Spring const. (N/m)	Frequency shift (kHz)	Effective no. of spores	Effective mass of a spore (fg)
L21	46.5	0.0275	1.2	2	492
R25	45.1	0.0355	2.9	7.12	324
R33	34.4	0.0632	4.5	3	528
R34	34.8	0.0604	2	2.94	215
R35	35.9	0.0602	5.1	6.7	250
R36	34.8	0.0682	3.7	6.08	222
R37	35.2	0.0683	9.6	5.74	623
R41	19.8	0.5874	6.7	1.856	371
R42	20.1	0.5900	10.8	2.9	443
R43	19.8	0.6313	28.5	7.94	414
R44	19.8	0.5700	4.1	1.54	296
R45	20.5	0.5256	7.3	3.74	226
Average mass (fg)					367.0
Standard deviation (fg)					134.73

(c)

Cantileve	Length (μm)	Frequency shift (kHz)	Effective number of spores	Effective mass of a spore (pg)
R41	20.1	2.82	10.192	1.92
R43	20.1	7.26	24.52	2.31
R45	20.5	2.9	14.82	1.36
R47	19.9	3.52	14.12	1.61
L44	20.9	2.58	20.16	0.845
L47	20.5	14.07	50.22	2.77
L48	21.6	31.18	147.06	3.17
L50	22	16.33	109.2	0.781
Average mass (pg)				1.85
Standard deviation (pg)				0.87

Cantilever width = 9 μm and cantilever thickness = 200 nm.

that there was an equal number on the top and bottom of the cantilever, so the effective number counted on the top was doubled. Furthermore, it was observed that not all the spores are identical in size (See the inset of Fig. 3); they do vary in length and diameter resulting in variations in mass. A *B. anthracis* spore is usually about 1.5–2 μm long and about 1 μm in diameter. Experiments were reported in the past to determine the mass of a *Bacillus cereus* spore to be about 1.5 pg (McCormick and Halvorson, 1964). Water content for spores varies by species and for *B. cereus*, a typical value was found to be 65% (Beaman et al., 1982). Assuming the spores in dry environment (after being subjected to critical point drying) experience 65% dehydration,

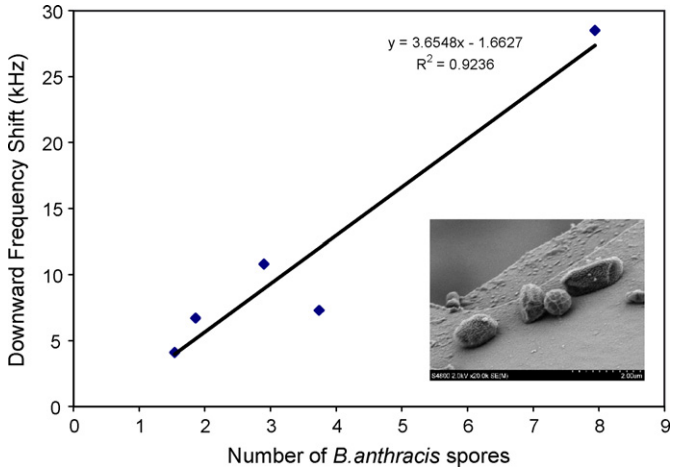

Fig. 3. Sensitivity of the 20 μm long cantilever showing the decrease in resonant frequency vs. the effective number of spores on the cantilevers, in air. The inset shows a close up SEM image depicting the non-uniformity in size of different spores.

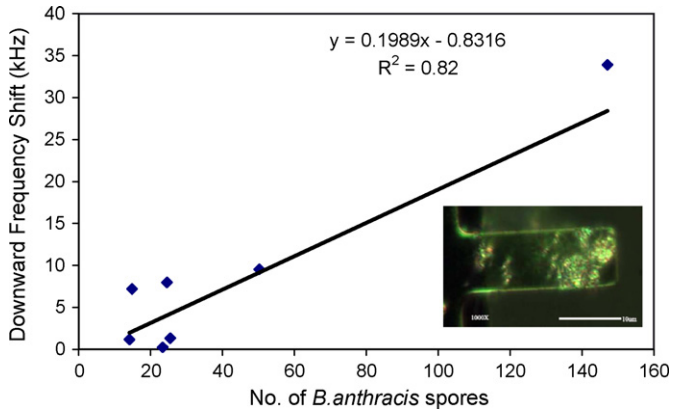

Fig. 4. Sensitivity of 20 μm long cantilevers in water. There is no linear dependence between the downward frequency shift and the effective number of spores below a count of 50 spores. This is due to the decrease of Q factor caused by high damping in the liquid. The inset shows a dark field photograph of a 20 μm long cantilever after measurements in water.

the mass of the spore would then be about 525 fg. The average mass of a single spore of *B. anthracis* according to our measurements was about 367 fg (See Table 1(b)), which is close to the expected value. It should be noted here that the method of counting spores results in uncertainties because it assumes that the same number of spores is located on the top and bottom, whereas there may not be the same number of spores underneath the cantilever because we used sedimentation to direct the spores floating in the suspension towards the cantilever surfaces.

The mass sensitivity of the cantilevers was also studied. The shift in the resonant frequency was obtained as a function of the effective number of spores. Fig. 3 demonstrates the sensitivity of the 20 μm long cantilevers for the measurement of spores in air and the mass sensitivity was calculated to be 9.23 Hz/fg from the linear fitting line. This linear relationship was obtained according to the first order approximation of the binomial series expansion of Eq. (1). The theoretical mass sensitivity was also obtained by dividing the minimum detectable frequency shift (Eq. (5)) by the minimum detectable mass, which is defined as the added mass to induce the minimum detectable frequency shift (Eq. (1)). The theoretical mass sensitivity was then calculated as 14.6 Hz/fg, which is in good agreement with the measurement. The minimum mass detected was approximately 740 fg corresponding to 2 spores, which is also in good agreement with the theoretical minimum detectable mass of 423 fg considering the measurement uncertainties.

3.5. Spore detection in water

To analyze the frequency spectra in water, the substrate noise was measured and subtracted from the thermal noise of the cantilevers. The resonant frequencies and quality factors were extracted from the filtered signal using Matlab software. The spores were imaged by SEM and the effective number of spores was counted for each of the cantilevers. Obviously, there were more spores on the surface of the cantilevers compared to the air measurements, which was needed because the sensor's sensitivity can be much reduced by the surrounding liquid.

Table 1(c) shows the mass results measured in water. The mass in the last column is the mass of a single spore obtained by dividing the total measured mass by the total effective number of spores. The frequency shift presented is the shift between the unloaded resonant frequency in water and the loaded resonant frequency with spores. The method of counting the spores was the same as used for the experiments in air. Consequently, there are uncertainties in the mass of a single spore for each cantilever. The average mass presented in Table 1(c) was 1.85 pg. This mass is in good agreement with the expected mass of 1.5 pg (McCormick and Halvorson, 1964) and also excludes the mass of the antibody and BSA layer. In addition, the mass of the antibody and BSA layer was calculated from the measured resonant frequency shifts in air and was an average of 0.1 pg (about 10% of the mass of the spore layer). It was observed that for cantilevers with a large number of spores, measurements with the LDV could not be performed (see Fig. S4). As a result, there was an upper limit for the number of spores that could be measured on the cantilever; that limit was not quantified in this experiment.

Fig. 4 shows the measured mass sensitivity of the cantilevers in water. Only the shortest cantilevers were suitable for these measurements. Moreover, as seen in Fig. 4, for an effective number of spores less than 50, the measured shift in frequency was almost independent of the number of spores, which was attributed to the decrease of the quality factor in a viscous medium. Therefore, the minimum number of spores that could be detected was about 50 spores among the tested spore numbers that correspond to a minimum detectable mass of about 140 pg, while the theoretical value was 224 pg using Eqs. (1) and (5). The sensitivity was measured to be 100 mHz/fg in water and the theoretical mass sensitivity was also calculated as 85 mHz/fg in the same way as described above. The agreement between measurements and experiments is quite close, given the experimental variability. Possible reasons for these discrepancies include the method of counting spores underneath the cantilevers by assuming that there is the same number of spores on the top and bottom.

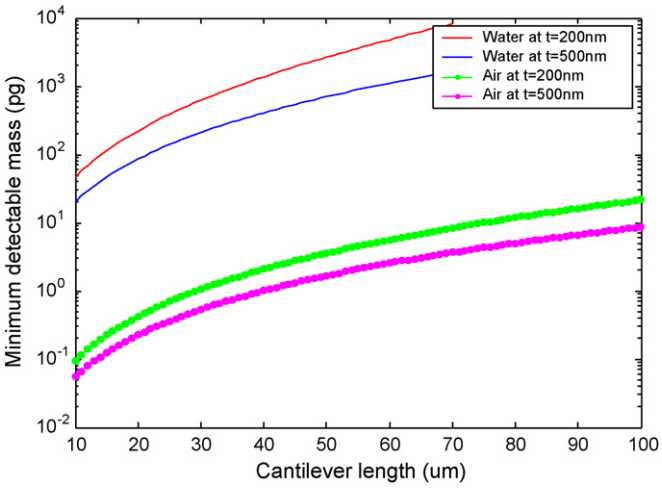

Fig. 5. Theoretical minimum detectable mass of thermal noise driven cantilevers in air and water. Cantilever width = 9 μm.

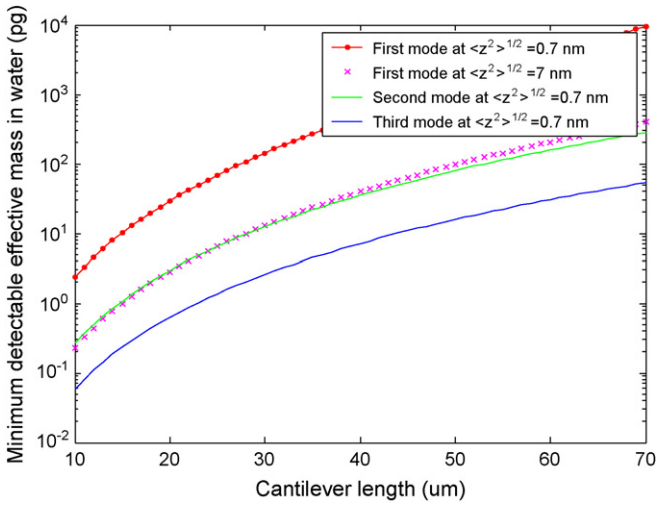

Fig. 6. Theoretical minimum detectable mass in water as a function of cantilever length for the first three flexural modes and different root-mean-square amplitudes of the cantilever that is constantly driven by piezoelectric material. Cantilever width = 9 μm and cantilever thickness = 200 nm.

In fact, there were much more spores in water case, implying that the uncertainties might increase compared to the air measurements. Another explanation may be that as shown in Fig. 4, there were not a sufficient number of data points between 50 spores and 140 spores, which was hard to control in the experiments.

3.6. Suggestions for improving cantilever performances in a viscous medium

In this work, we demonstrated that it is possible to detect the presence of as few as about 50 spores using optimized cantilevers with a simple planar geometry in liquid, even with a thermal noise source, i.e., without intentionally driving the cantilevers. The minimum detectable mass and mass sensitivity depend on the material properties of the surrounding media, cantilever size and shape, etc. As for the material properties of surrounding media, they are mostly affected by the viscosity as described in Sections 3.1 and 3.3. For a given medium, a cantilever size should then be optimized for better performance. Fig. 5 shows the minimum detectable mass in air and water as a function of the cantilever length using the SHO model (Sader, 1998) and Eqs. (1) and (5). As shown in the graph, the shorter and thicker cantilevers are more desirable. In fact, according to the current measurements, the shorter cantilevers were more sensitive, exhibiting a larger frequency shift. However, it should be noted that this SHO model is known to be inaccurate for cantilevers with the length to width ratio less than 4. Considering the quality factors shown in Fig. 1, the minimum detectable mass could be larger than the theoretical predictions. Also, as the thickness increases, the minimum detectable mass decreases while the resonant frequency increases linearly, requiring larger measurement bandwidth. Moreover, the rate at which the minimum detectable mass decreases with thickness becomes smaller with thicker cantilevers, so the effects of the thickness on the minimum detectable mass become smaller as the cantilevers become thicker.

For a given geometry of cantilevers and surrounding media, the minimum detectable mass can be improved using higher order harmonic frequencies. These might be favorable for long cantilevers, which show small quality factors or small fundamental resonant frequencies. The minimum detectable mass can also be reduced by increasing the cantilever amplitude by externally driving the cantilever. Fig. 6 shows the minimum detectable mass as a function of cantilever length for the first three modes of harmonics and different root-mean-square (rms) amplitudes of the cantilevers. The minimum detectable frequency shifts for the second and third modes were obtained by replacing the spring constant in Eq. (5) with the mode-dependent spring constant (Rast et al., 2000; Ono et al., 2005). The minimum detectable mass decreases with the increasing cantilever amplitudes and increasing modes. In fact, the minimum detectable mass decreases approximately by 10^2 times as the flexural mode changes from the first to the third with constant cantilever amplitudes, which can make possible single spore detection in liquid. For example, the minimum detectable mass for 20 μm long cantilevers is calculated as 0.63 pg, about a half of single spore mass, at the third mode of harmonics and an rms cantilever amplitude of 0.7 nm.

4. Conclusions

We presented detection of *B. anthracis* Sterne spores in air and water using micro resonant cantilevers. The resonant frequencies due to thermal noise excitation were measured using a LDV to find an added mass on the cantilevers. A minimum of 2 spores (740 fg) and 50 spores (139 pg) can be detected in air and water, respectively, with 20 μm long, 9 μm wide, and 200 nm thick cantilevers. We also compared the measurements with theoretical predictions based on the SHO model and comparisons showed a good agreement between them. This study demonstrated the ability to perform mass detection of a biological organism in a viscous medium using micro resonant mass sensors of simple planar geometry, even with thermal noise excitation. Further improvement of cantilever sensitivity can be

achieved by observing higher order harmonics or by externally exciting cantilevers to higher amplitudes, whereby single spore detection in liquids should be attainable.

Acknowledgments

A. Davila was supported by the NASA Institute of Nanoelectronics and Computing at Purdue through a fellowship. The work was also supported by NIH R21 AI053683-01 (NIAID) to R. B. and A. A. The authors are thankful for the financial support of the US National Institute of Health (NIBIB grant number R21/R33 EB00778-01) for funding Dr. Jaesung Jang. The authors would like to thank Hung Chang, Oguz Elibol and Chia-Ping for taking the SEM micrographs of the cantilevers, and the staff of the Birck Nanotechnology Center for fabrication support.

Appendix A. Supplementary data

Supplementary data associated with this article can be found, in the online version, at doi:10.1016/j.bios.2007.01.012.

References

Beaman, T.C., Greenamyre, J.T., Corner, T.R., Pankratz, H.S., Gerhardt, P., 1982. J. Bacteriol. 150, 870–877.
Braun, T., Barwich, V., Ghatkesar, M., Bredekamp, A., Gerber, C., Hegner, M., Lang, H., 2005. Phys. Rev. E 72, 031907.
Burg, T., Manalis, S., 2003. Appl. Phys. Lett. 83, 2698–2700.
Burtscher, C., Wuertz, S., 2003. Appl. Environ. Microbiol. 69, 4618–4627.
Campbell, G.A., Mutharasan, R., 2006. Biosens. Bioelectron. 21, 1684–1692.
Chen, S., 1987. Hemisphere Pub Corp., Washington.
Chon, J.W.M., Mulvaney, P., Sader, J.E., 2000. J. Appl. Phys. 87, 3978–3988.
Chu, W.-H., 1963. Technical Report No. 2, DTMB Contract Nobs-86396(X). South-West Research Institute, San Antonio, TX.
Ekinci, K.L., Yang, Y.T., Roukes, M.L., 2004. J. Appl. Phys. 95, 2682–2689.
Gfeller, K., Nugaeva, N., Hegner, M., 2005. Biosens. Bioelectron. 21, 528–533.
Gupta, A., Akin, D., Bashir, R., 2004a. J. Vac. Sci. Technol. B 22, 2785–2791.
Gupta, A., Akin, D., Bashir, R., 2004b. Appl. Phys. Lett. 84, 1976–1978.
Ilic, B., Czaplewski, D., Zalalutdinov, M., Craighead, H.G., Neuzil, P., Campagnolo, C., Batt, C., 2001. J. Vac. Sci. Technol. B 19, 2825–2828.
Ivnitski, D., Abdel-Hamid, I., Atanasov, P., Wilkins, E., 1999. Biosens. Bioelectron. 14, 599–624.
Kirstein, S., Mertesdorf, M., Schönhoff, M., 1998. J. Appl. Phys. 84, 1782–1790.
Landau, L.D., Lifshitz, E.M., 1959. Pergamon, London.
Lavrik, N.V., Sepaniak, M.J., Datskos, P.G., 2004. Rev. Scientific Instrum. 75, 2229–2253.
McCormick, N., Halvorson, H., 1964. J. Bacteriol. 87, 68–74.
Nugaeva, N., Gfeller, K., Backmann, N., Lang, H., Düggelin, M., Hegner, M., 2005. Biosens. Bioelectron. 21, 849–856.
Ono, T., Lin, Y.-C., Esashi, M., 2005. Appl. Phys. Lett. 87, 074102.
Prescesky, S., Parameswaran, M., Rawicz, A., Turner, R., Reichl, U., 1992. Can. J. Phys. 70, 1178–1183.
Prescott, L.M., Harley, J.P., Klien, D.A., 2005. McGraw-Hill, Dubuque, IA.
Rast, S., Wattinger, C., Gysin, U., Meyer, E., 2000. Nanotechnology 11, 169–172.
Sader, J.E., 1998. J. Appl. Phys. 84, 64–76.
Sader, J.E., Chon, J.W.M., Mulvaney, P., 1999. Rev. Scientific Instrum. 70, 3967–3969.
Walters, D.A., Cleveland, J.P., Thomson, N.H., Hansma, P.K., Wendman, M.A., Gurley, G., Elings, V., 1996. Rev. Scientific Instrum. 67, 3583–3590.